Two global maps of anthropogenic CO_2 emission derived using database of large point source

Tomohiro Oda and Shamil Maksyutov
Center for Global Environmental Research, National Institute for Environmental Studies
16-2 Onogawa, Tsukuba, Ibaraki 305-8506 Japan
oda.tomohiro@nies.go.jp

ABSTRACT

We developed two types of global maps at a resolution of 5 km of anthropogenic CO_2 emission using a database of major CO_2 point sources. In the present study, CO_2 emission from major point sources was subtracted from national total emission which is calculated from an energy consumption statistics. Emissions from point sources were directly mapped, and emissions from non-point sources were distributed based on population statistics and satellite-observed nighttime lights data which indicate human settlements and gas flares. Population statistics can locate emissions reasonably and explain the intensity of human activities. On the other hand, the use of the nighttime lights data is a more reliable way to locate emissions. We also derived a temperature-energy demand relationship to parameterize seasonality of CO_2 emission and the relationship can be used for calculating monthly emissions from annual total emissions. We created global emission maps for the period between 1980 and 2007 using weighting factors calculated from the normalization of total global emission.

1. INTRODUCTION

Inventory of atmospheric constituent is a basic data for atmospheric modeling. CO_2 inventory has been used as an input for forward transport modeling which gives an interpretation to atmospheric CO_2 measurements. Inversion of atmospheric CO_2, which is a calculation to estimate surface source/ sink of CO_2 using atmospheric modeling (e.g. Gurney *et al.*, 2002), also requires the inventory as a reference to look at CO_2 remaining in the atmosphere and a balance of anthropogenic, biospheric and oceanic fluxes.

Global map of anthropogenic CO_2 has been developed in previous studies (e.g., Marland *et al*., 1984; Boden *et al*., 1995; Andres *et al.,* 1996). They calculated global and national CO_2 emissions by integrating statistics of energy consumption and cement manufacture as well as international trade statistics. They used population statistics as a surrogate in order to distribute emission to source regions. This is a reasonable procedure since population data have reasonable spatial resolution of the country and city levels. On the other hand, population statistics do not explain emissions from point sources such as power plants and heavy transportations. Since density of population is directly related to the intensity of emission, intense point sources may not appear on an emission map, and thus emission at a location where a point source exists can be underestimated. In addition, population statistics do not map emissions to the exact locations of sources if the map resolution is smaller than city level. As human settlement is not uniform within a region, emission might be distributed to areas where people actually do not live.

In this study, we developed global emission maps using a database of major point sources in order to treat emission from point sources separately. We created the two global maps using two different location/intensity surrogates that are based on population count and satellite-observed nighttime lights data that indicate human settlements and gas flares. We also derived a temperature-energy demand relationship to parameterize seasonality of CO_2 emission to calculate monthly emissions from annual total emissions. We created global emission maps for the period between 1980 and 2007 using weighting factors calculated from the normalization of total global emission.

2. DATA AND METHODOLOGY

2.1. National and Regional CO_2 Emission

Estimates of annual national CO_2 emissions obtained in the present work are based on worldwide energy statistics compiled by BP plc. (web resource, 2009 (http://www.bp.com/productlanding.do?categoryId=6929&contentId=7044622)). The statistics, which covers the period between 1965 and 2007, indicates the consumption of commercially traded primary fuels (oil, coal, and natural gas) in 65 countries and administrative regions. Consumption of such fuels in six major geographical regions are also provided to show the statistics of countries or regions that are not included in the above data. The six regions are denoted as North America, South and Central America, Europe and Eurasia, Middle East, Africa, and Asia Pacific. The coverage of each region is shown in Figure 1. In this work, annual CO_2 emissions for 71 regions (65 nations and regions as well as the six major regions) are computed from the consumption statistics of oil, coal, and natural gas. The oil statistics covers all inland demands, international airborne and maritime transports, and refinery fuel and losses. Consumption of fuel ethanol and biodiesel are included as well. The coal statistics refer only to the amounts of solid fossil fuels such as bituminous coal, anthracite (hard coal), lignite, and brown (sub-bituminous) coal.

The CO_2 emissions are estimated via calculating the carbon content of the consumed fuels. The calculation is done in a stepwise manner and is explained as follows. Conversion factors used in the calculation are, if not specified otherwise, adopted from the 2007 statistics report prepared by the

Figure 1. Six major geographical regions as defined in the BP worldwide energy statistics (BP plc., 2009).

International Energy Agency (IEA, 2007). The quantities of nationally and regionally consumed primary fuels in the BP statistics (in million tonnes of oil equivalent per year) are first converted into energy amount in terajouls. The amount of natural gas in the statistics is given in billion cubic meters, and a conversion factor of 0.90 is applied to express the amount in million tonnes of oil equivalent. The energy amounts obtained are then used to compute the carbon content of the consumed fuels. The following carbon emission factors (CFE, in tonnes of carbon per terajouls) are applied: 15.3 (natural gases); 26.4 (coal); 20.0 (oil). The CFE for coal adopted here is an average of CFEs for anthracite, coking coal, other bituminous coal, sub-bituminous coal, and lignite. To account for the fractions of carbon unoxidized in the combustion of the fuels, correction factors of 0.99 (oil), 0.98 (coal), and 0.995 (natural gas) are applied. The annual estimate of national/regional CO_2 emissions from primary fuel combustion are then found by multiplying the remaining carbon amounts by 44/12, which is the molecular weight ratio of CO_2 to carbon.

Our estimation procedure parallels with the methodology shown in the revised IPCC 1996 guidelines for National Greenhouse gas inventories (IPCC, web resource, 2009 (http://www.ipcc-nggip.iges.or.jp/public/gl/invs1.html)), except in the estimation of national fuel consumptions. In the reference approach of the revised 1996 IPCC guidelines, the amount of total fuel supplied, denoted as apparent consumption, is the basis of the national carbon supply calculation, and is calculated as a sum of the produced and imported amounts subtracted by the amounts for international bunkers and stock changes. We compare our estimations with those obtained via other approaches later in Section 2.2.

2.2. CO_2 emissions from point sources and non-point sources

Among the known point sources, fossil fuel-fired power plants are the major contributors to the annual national or regional CO_2 emissions. Records of emissions from power plants worldwide are available in a database, thus emissions from diffuse non-point sources in a nation or a region can be loosely approximated by subtracting the emissions of power plants from the national total emission. These approximations can be used in analyzing the locations and the strengths of the non-point sources. The diffuse non-point sources include residential and commercial heating and cooling as well as daily land transportations. They can be recurring but are not as strong and persistent as point sources. Although weak and widespread, the strengths of non-point sources may be well correlated with the local human activities and thus the local population. Population statistics can be used to infer the geographical distributions of human activity intensity. Thus, redistributing the national estimate of non-point source emissions according to such activity intensity yields a distribution of non-point source emissions. The data can be superimposed onto the distribution of point source emissions, which can be constructed with the power plant emission records. Global distribution of both point and non-point sources is obtained.

In this work, we utilize a database CARMA (Carbon Monitoring and Action, web resource, 2009 (http://carma.org)) to obtain locations and emissions of power plants worldwide. Figure 2 shows the locations of power plants listed in CARMA database. For population statistics, Gridded Population of the World version 3 (GPWv3), a dataset provided by the Center for International Earth Science Information Network at Columbia University, NY, USA, is used. GPWv3 depicts the distribution of human population across the globe at a resolution of 2.5 arc minute (approximately 5 km). The GPWv3 data for 2005 and the accompanied national boundary data for 2000 are used in this study. Each population count within a grid is normalized to the national or the regional total. The normalized population counts are then used as weighting factors when redistributing national non-point emissions.

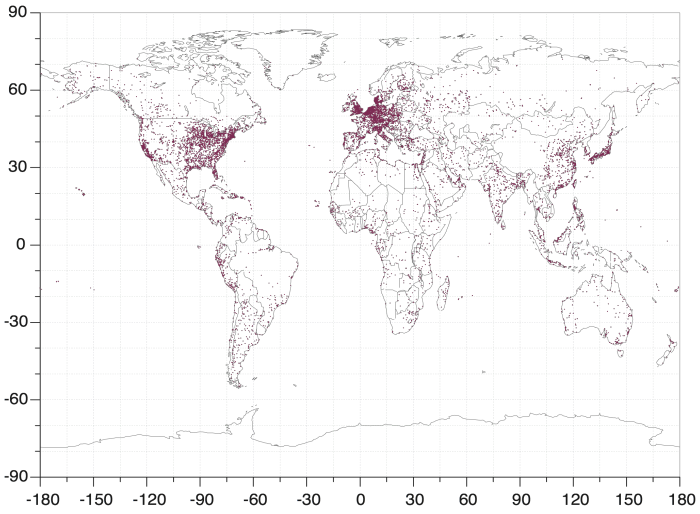

Figure 2. Power plants listed in CARMA database. Only the power plants with confirmed location information are shown.

Also adopted in this study is a dataset of satellite-observed nighttime lights, a product provided by the Defense Meteorological Satellite Project (DMSP) of the US National Oceanic Atmospheric Administration (NOAA). The stable lights data, which are products of the nighttime lights data processed to exclude fires, gas flares, and fishing boats, are utilized in this study. This data can indicate the locations of human settlements and activities such as daily land transportations, which do not appear in population distributions. With the stable lights data, non-point sources can be located more precisely. For this study we use the stable lights data for the 1994-1995 period. The original data resolution of 1 arc minute is relaxed to 2.5 arc minute via interpolation. As in the use of GPWv3 data, gridded light occurrences are normalized to the national or regional total.

2.3. Seasonality of CO_2 Emission

Electricity demands are weather sensitive and highly dependent on cooling and heating needs of both the residential and commercial sectors. The cooling and heating needs varies with change of seasons thus corresponding variation in electricity consumption is linked to the seasonality of CO_2 emission. Simple models have been developed for predicting electricity demands based on weather variables such as local ambient air temperature, wind speed, and humidity. A regression model of Sailor and Vasireddy (2005) predicts changes in the average monthly regional electricity demands in terms of varying temperature. The model is formulated with heating degree days (HDD) and cooling degree days (CDD), which are indices of energy demand for heating or cooling a space with respect to ambient temperature. HDD and CDD are defined as differences between the daily mean temperatures above or below a base temperature that depends on local climate patterns. The model is formulated as:

$$EL = A + B \times CDD + C \times HDD, \qquad (1)$$

where *EL* is the average monthly regional electricity demand, *A*, *B*, and *C* are regression coefficients, and *CDD* and *HDD* are the cooling and heating degree days of the region. The regression constants are determined by training the model with historical records of regional monthly electricity consumption and corresponding CDD and HDD for a certain duration. As suggested in Sailor and Vasireddy (2005), the model calculations can be simplified by setting the cooling degree day coefficients (*B* in Equation 1) to zero for winter (low temperature) period (January-March and October-December), and setting the heating degree day coefficients (*C* in Equation 1) to zero during summer (April-September).

In the present work, we attempt to use this model to attain global relationship between total monthly CO_2 emission and monthly average temperature. This model was originally developed to predict intrastate and city-scale energy demand in the US. We extend the capability of the model to obtain global maps of monthly CO_2 emissions. In brief, this is achieved via obtaining a population-weighted intrastate relationship between monthly state electricity consumption and monthly state average temperature for all 50 states of the US. We then aggregate these local state relationships to obtain the population-weighted national representative relationship. The meridional coverage of the 50 states ranges from temperate, subtropical Florida and Hawaii to boreal, arctic Alaska, representing nearly all types of regional climate patterns on the globe. We will use this US national relationship to obtain global maps of monthly electricity consumption based on global monthly average temperature distribution. We then finally infer worldwide monthly CO_2 emissions via weighting the global distribution of annual CO_2 emission, which is prepared by the method discussed earlier, with factors calculated from the global monthly electricity consumptions.

Data needed to train individual state electricity demand models include monthly electricity consumptions in mega watts hour per capita and population-weighted monthly CDD and HDD for all the 50 states. We use the monthly electric utility sales and revenue data, which are provided by the US Energy Information Administration (web resource, 2009 (http://www.eia.doe.gov/cneaf/electricity/page/eia826.html)), to obtain electricity consumptions in the 50 states. In this study we use the data for residential sectors. The monthly CDDs and HDDs as well as monthly state average temperatures are provided by the National Climatic Data Center of NOAA (web resource, 2009 (http://www.ncdc.noaa.gov/oa/documentlibrary/hcs/hcs.html#51overview)). Individual state models are trained over the 2003-2006 period. Linear regression analyses are performed to attain the electricity demand-temperature relationships.

3. RESULTS AND DISCUSSION

3.1. National and regional CO_2 emission

The estimates of national and regional CO_2 emission for 2006 are presented in Table 1 and Figure 3. Table 2 and Figure 4 show the emissions in six major geographical regions. For 61 nations and regions included in BP statistics, CO_2 emission from point sources accounts for a substantial proportion of the total emission. It accounts for nearly half of the total emission for several countries (e.g., Australia, Germany, India, Poland and South Africa). This supports the idea that the procedure in which national and regional total emission is distributed, can cause underestimation of CO_2 emission at a location where point sources exist.

Since the major six geographical regions are aggregated categories of countries and regions that are not included in BP statistics, we assumed that countries and regions included in a region have the same proportion of CO_2 emission from point sources and non-point sources. The proportion of point-

source emission in the total emission seems to be smaller than the proportion of point sources for 61 countries and regions. This might be because most industrial countries and regions are included in 61 countries and regions above. However, CO_2 emission from point sources for six geographical regions still accounts for a negligible proportion of the total emission.

Table 1. National and regional annual emissions based on the BP statistics. (in million tonnes of CO_2 per year).

Country and code		Total	Point sources	Non-point sources
United Arab Emirates	ARE	784.000	15.108	134.887
Argentina	ARG	153.414	28.747	124.667
Australia	AUS	402.611	196.241	206.370
Austria	AUT	74.097	15.967	58.130
Azerbaijan	AZE	34.735	8.850	25.886
Belgium*	BEL	593.432	130.617	462.815
Bangladesh	BGD	48.284	7.848	40.436
Bulgaria	BGR	51.231	24.527	26.705
Belarus	BLR	62.478	13.310	49.168
Brazil	BRA	370.632	15.136	355.495
Canada	CAN	630.085	159.692	470.393
Switzerland	CHE	44.963	0.242	44.720
Chile	CHL	66.684	16.437	50.247
China	CHN	6023.010	2601.429	3421.581
Colombia	COL	57.072	8.469	48.604
Czech	CZE	127.727	58.079	69.648
Germany	DEU	891.467	407.226	484.241
Denmark	DNK	61.411	24.134	37.277
Algeria	DZA	87.684	16.538	71.146
Ecuador	ECU	24.372	2.122	22.251
Egypt	EGY	152.165	41.853	110.312
Spain	ESP	381.966	113.692	268.274
Finland	FIN	61.538	31.323	30.215
France	FRA	423.308	25.926	397.382
United	GBR	607.282	218.724	388.558
Greece	GRC	106.171	49.256	56.915
Hong Kong**	HKG	79.053	0.000	79.053
Hungary	HUN	61.357	15.874	45.483
Indonesia	IDN	332.136	73.634	258.501
India	IND	1220.412	559.148	661.264
Ireland	IRL	45.519	15.327	30.192
Iran	IRN	466.456	71.056	395.400
Iceland	ISL	3.231	0.003	3.229
Italy	ITA	494.924	146.516	348.408
Japan	JPN	1371.236	373.438	997.799
Kazakhstan	KAZ	189.148	49.335	139.813
Republic of Korea	KOR	613.871	150.564	463.306
Kuwait	KWT	69.698	5.216	64.482
Lithuania	LTU	16.298	0.898	15.401
Mexico	MEX	408.379	98.172	310.207
Malaysia	MYS	160.625	54.764	105.861
Netherlands	NLD	263.143	58.358	204.785
Norway	NOR	41.287	0.753	40.534
New	NZL	38.093	8.281	29.812
Pakistan	PAK	134.142	19.950	114.192
Peru	PER	24.899	4.370	20.529
Philippines	PHL	68.253	31.469	36.784
Poland	POL	330.578	152.960	177.618
Portugal	PRT	67.411	23.644	43.766
Qatar	QAT	51.574	5.096	46.478
Romania	ROU	103.451	0.000	103.451
Russian	RUS	1680.534	448.475	1232.059
Saudi	SAU	436.469	52.239	384.230
Singapore	SGP	147.892	4.794	143.098
Slovakia	SVK	39.113	10.226	28.887
Sweden	SWE	61.693	2.774	58.918
Thailand	THA	231.425	59.901	171.525
Turkmenistan	TKM	53.686	4.823	48.864
Turkey	TUR	271.861	79.978	191.883
Taiwan**	TWN	338.018	106.863	231.155
Ukraine	UKR	344.964	67.563	277.401
United States	USA	6410.942	2804.882	3606.060
Uzbekistan	UZB	112.449	30.598	81.852
Venezuela	VEN	138.939	11.397	127.542
South Africa	ZAF	449.763	218.134	231.629

(Unit: million tonnes CO2/year)

* Belgium includes Luxembourg

** Administrative region

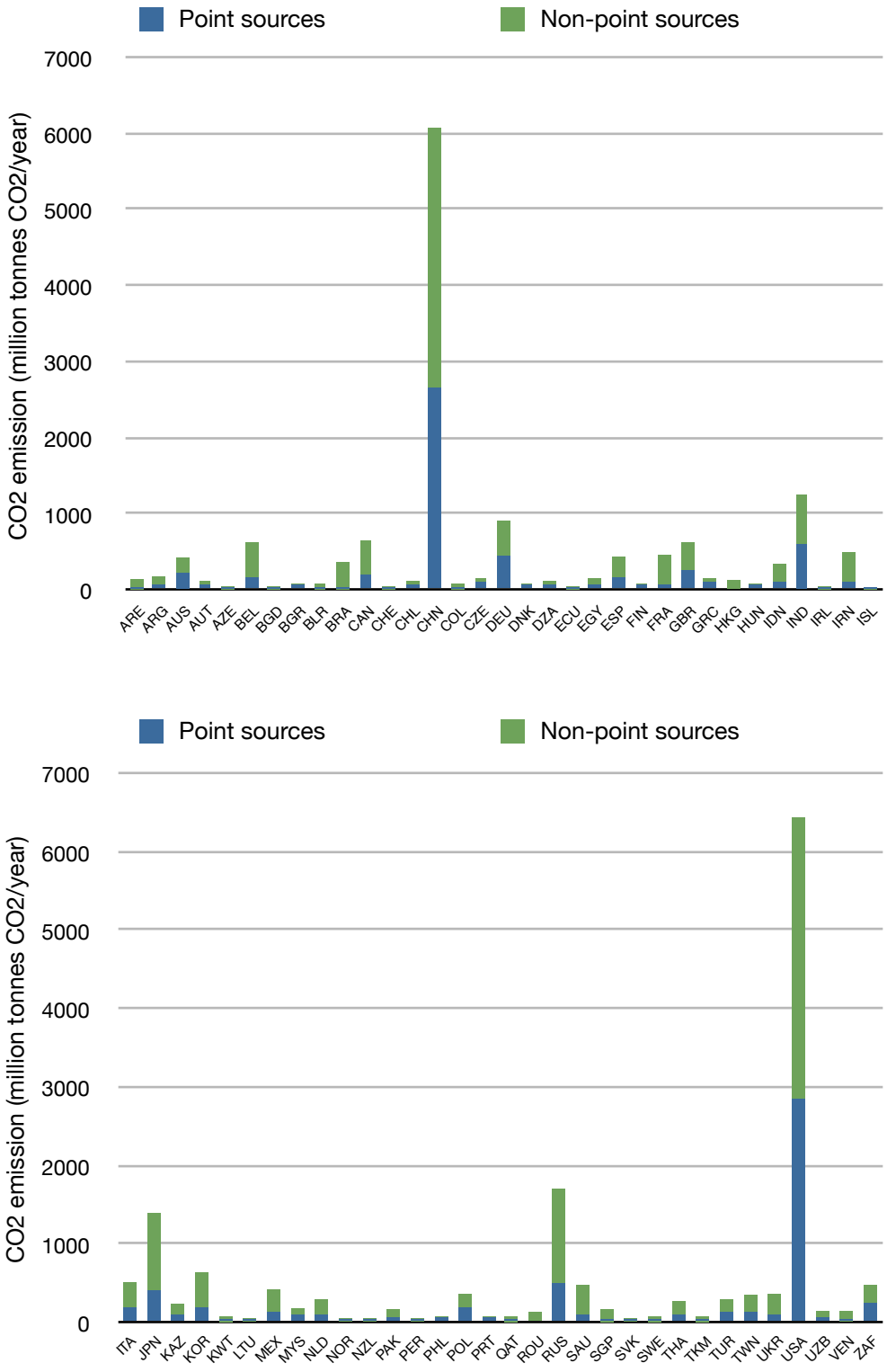

Figure 3. Estimates of national and regional total CO_2 emission. Blue and green portions indicate contributions from point sources and non-point sources, respectively (in million tonnes of CO_2 per year).

Table 2. Estimates of CO_2 emissions in the six major geographical regions (in million tonnes of CO_2 per year).

Region	Total	Point sources	Non-point sources
North America	0.319	0.316	0.003
S. & Cent. America	253.199	24.241	228.958
Europe & Eurasia	195.601	62.573	133.028
Middle East	330.007	79.832	250.174
Africa	281.451	56.939	224.511
Asia Pacific	244.953	26.376	218.577

(Unit: million tonnes CO2/year)

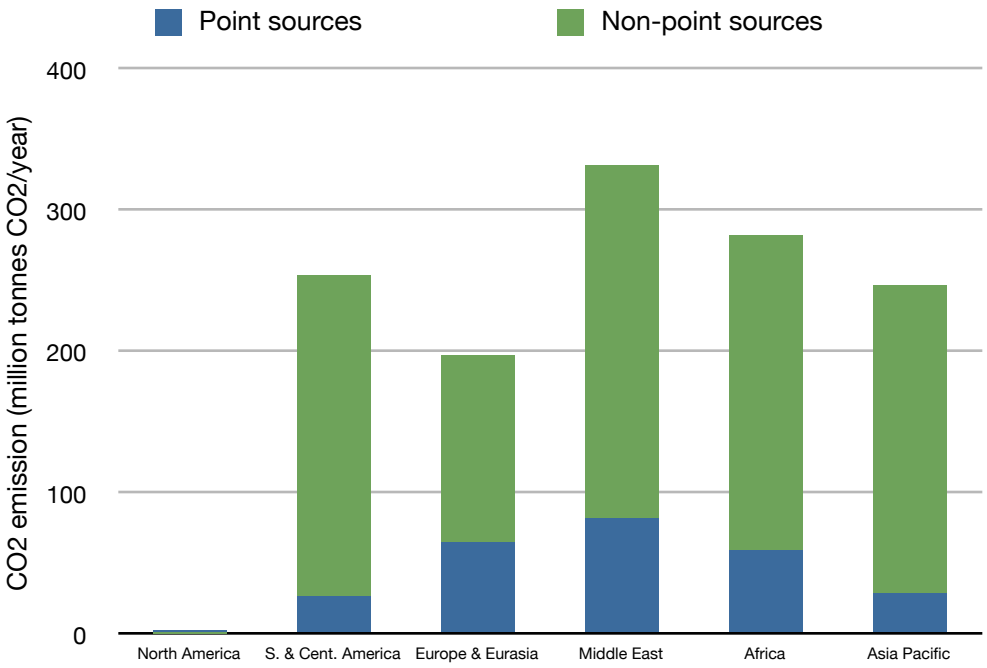

Figure 4. Estimates of total CO_2 emissions in the six major geographical regions. Blue and green portions indicate contributions from point sources and non-point sources, respectively (in million tonnes of CO_2).

3.2. Comparison with other inventories

To validate CO_2 estimates in this study, we compared the estimates with inventory estimates by CDIAC (Marland *et al*., 2008) and IEA (2007) (Figure 5). CDIAC and IEA were developed in procedures which are different from our procedure. CDIAC estimate was derived from energy statistics

published by United Nation (U.N., 2006) according to a procedure described by Marland and Rotty *et al.* (1984). On the other hand, IEA procedure parallels with the methodology shown in the revised IPCC 1996 guidelines and IEA provides two types of estimates (reference approach and sectoral approach).

Reference approach begins with calculation of total energy consumption as described in section 2.1 and in sectoral approach, national estimates was developed by compiling national sectoral emission statistics. In IPCC framework, reference approach is used for verification of inventory developed using sectoral approach. Here, we selected sectoral approach estimate for comparison, that is fairly different from our procedure. We selected top 5 countries in CO_2 emission (Unites States, China, Russia, India and Japan) from CDIAC and IEA for 2005 and compared with our estimates. Since our estimates were calculated for 2006, it was adjusted to 2005 using weighting factors calculated from the normalization of total global emission described later in this section.

The difference between our estimate and CDIAC estimate could be explained by the differences in calculation procedures. Our estimates was derived from energy consumption that includes consumption from international bunkers while CDIAC excluded it. Also, energy amount that accounts for export/import and stock change, which is considered in calculation of apparent consumption, was not considered in our procedure. The difference between our estimate and IEA estimate is largely due to the difference in the calculation approaches. The revised IPCC 1996 guidelines suggested that CO_2 emission estimates which are developed by sectoral and reference approaches match with difference of approximately 5% in condition of data is appropriate (e.g. quality and quantity of data). Thus, our estimate was reasonable considering the existing differences.

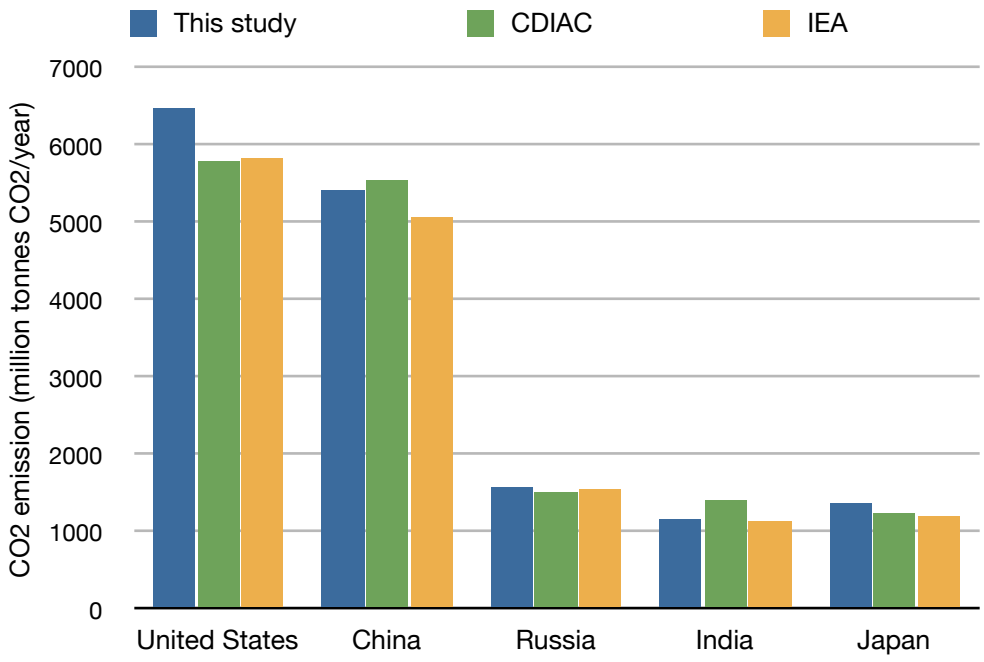

Figure 5. Estimated CO_2 emission amount of the world's five major source countries (in million tonnes of CO_2 per year). The IEA estimates are based on the sectoral approach.

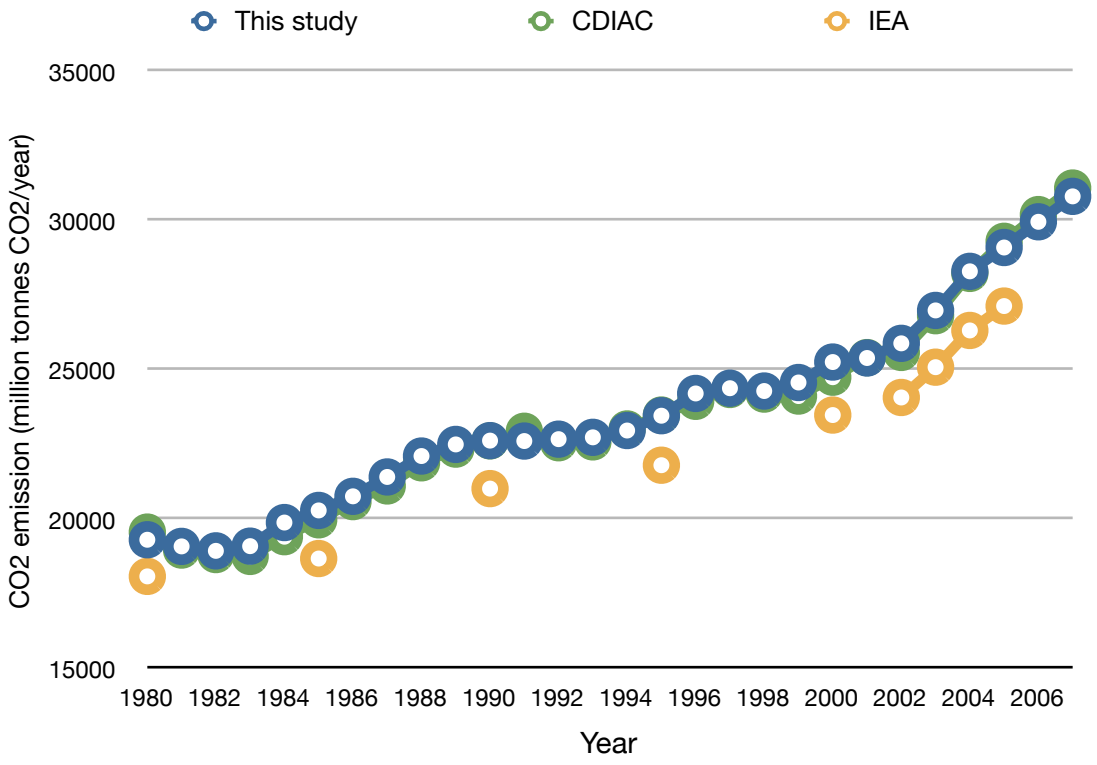

Figure 6. Comparison with CDIAC and IEA estimates (in million tonnes of CO_2 per year).

We also compared our global estimates with the two inventories (Figure 6). Our estimate shows good agreement with CDIAC. This is because the differences in calculation procedures for global estimate (e.g. consumption statistics and conversion factors) are minor compared to the difference found in the procedures for national estimates (e.g. import/export and stock change). Our estimate seems to be overestimate compared to IEA estimate, however the difference from IEA appeared to be around acceptable level of approximately 5%. In this study, we did not calculate national and regional emissions every year. National and regional emission for 1980-2007 was derived from estimates for 2006 by applying weighting factors which are obtained by normalizing annual global estimates for each with estimate for 2006. In this study, we assumed that the trend of national and regional emission are the same as the global trend and obtained 28-year emissions.

3.3. Global CO_2 emission maps

Global maps created with population and satellite-observed nighttime surrogates are shown in Figure 7 and 8, respectively. Both maps indicate major cities as intense source areas which have emissions on the order of ten million tonnes CO_2 per year (e.g. Los Angels, Paris, Moscow, Seoul and Tokyo). Our emission estimates for major cities might be smaller than estimates in other studies. This is

because emission from point-sources was subtracted before distributing using surrogates in this study. Since point source emissions were directly mapped, source regions can be seen in the region which are not residential areas.

On the map created with population surrogate (Figure 7), we still can see the national and administrative boundaries which seem to be artificial. This might be because the resolution of the population data was not enough to resolve city or smaller level for some areas since original population survey is not reported at such resolution. Especially in desert areas and mountainous areas, regions that have uniform weak CO_2 emission can be found. They seem unlikely to be source regions with uniform weak emission as indicated in the map. The emission should be distributed to other regions or mapped to exact locations of point source or human settlements. However, this is beyond the ability of population surrogate.

The map created with nighttime lights surrogate shows fairly different distribution of CO_2 emission compared the map created with population surrogate. Intense source areas can be seen at major cities and even at locations which are not major cities. Also, the map does not have unnatural uniform source regions which were found in the population surrogate map. Basically the stable lights indicate human settlements and gas flares. However, it seems to be able to indicate interstate highway in United States and major roads in other countries or regions. The map might indicate line sources attributed to heavy transportations. Thus, the nighttime lights surrogate have a great advantage of mapping CO_2 emission to possible locations. But the nighttime lights does not have enough information to explain the difference in emission strength among source regions since the nighttime lights data was provided as occurrences of detectable lights. The differences can be seen among the source areas are largely explained by the differences among total emissions for countries and regions where the areas belong to, if the occurrence is the same. The source strength also depends on the national and regional total number of lights. Total CO_2 emission of United States is larger than that of China, however lights in China were more colored in red than Unites States because of large CO_2 emission and the small number of lights indicating source regions. The same explanation can be done for small countries with large emission such as Netherlands, Belgium and several countries and regions in Middle East and Asia.

3.4. Global Temperature-Energy Relationship

We derived a global relationship of temperature and energy demand to create monthly emission from annual total emission. The energy demand prediction model, which was used to obtain model estimates of state energy demand, was successfully calibrated using state energy energy consumptions which were calculated from the monthly electric utility sales and revenue data. We tested model performance by reconstructing energy consumption data using CDD/HDD data. After model evaluation, we calculated energy demand for 2003-2006 and performed linear regression to derive a energy demand function of temperature. The model estimates of state energy demand were normalized by the averages of state energy demand. And the normalized energy demand estimates were integrated with monthly temperature data. The integrated data was divided into two parts by the threshold temperature of 65 degree F and linear regression was performed for each part. We obtained a pair of gradients for each state and then, we derived a pair of aggregated gradients by calculating population-weighted average.

The derived global energy function of temperature is shown in Figure 9. Solid purple and blue lines and solid red consist of a global curve. Gray open circle shows energy demand statistics used for

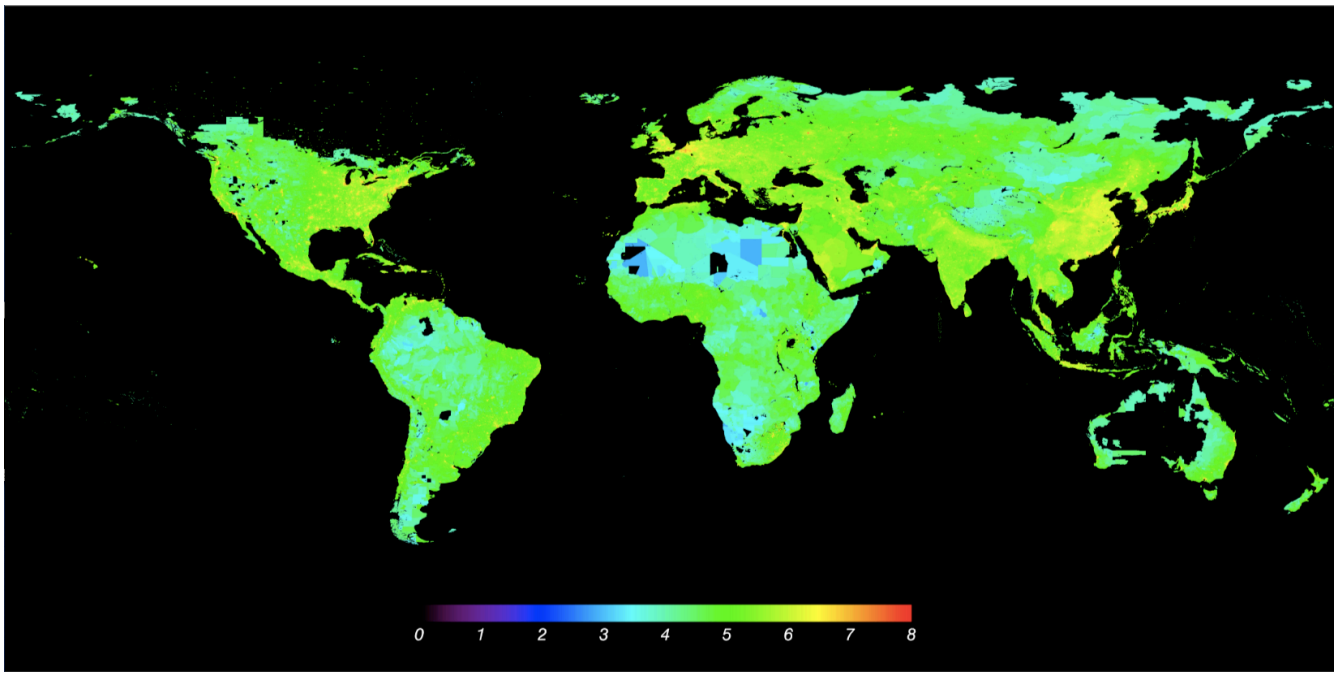

Figure 7. Global map of CO_2 emissions in 2006 based on the population statistics (in log base 10 tonnes of CO_2 per year).

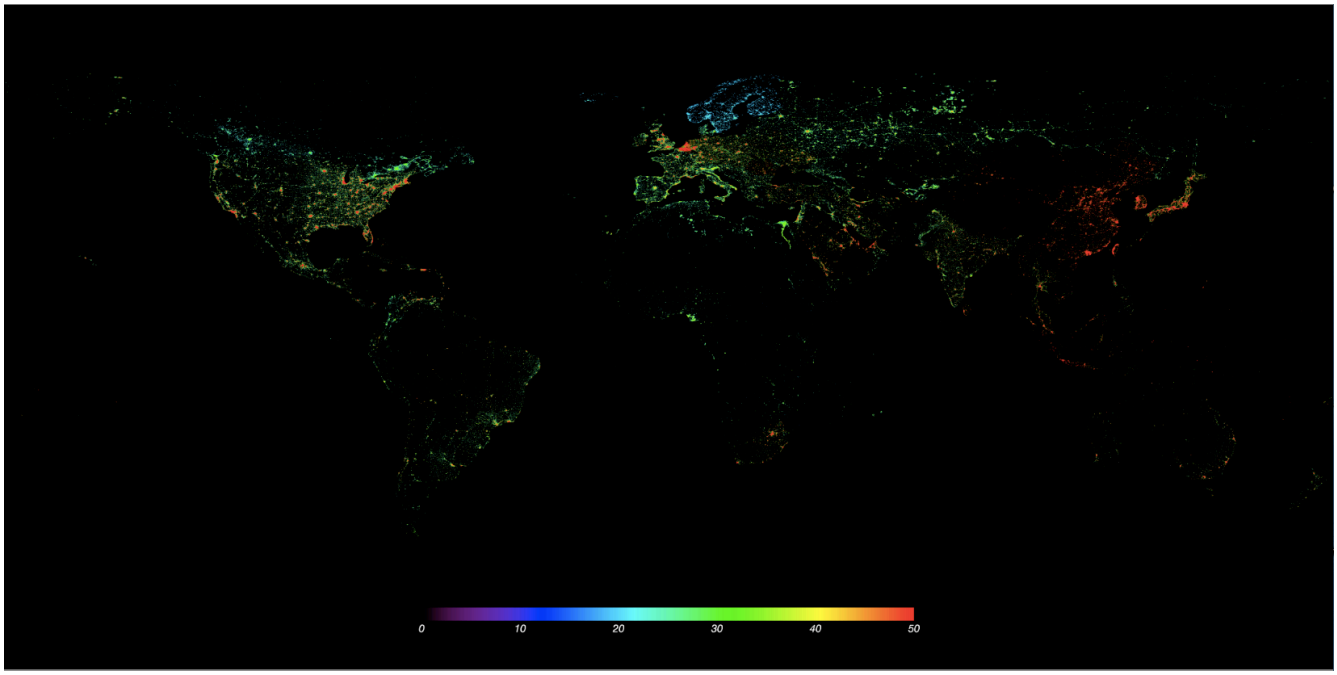

Figure 8. Global map of CO_2 emissions in 2006 based on the stable lights data (in million tonnes of CO_2 per year).

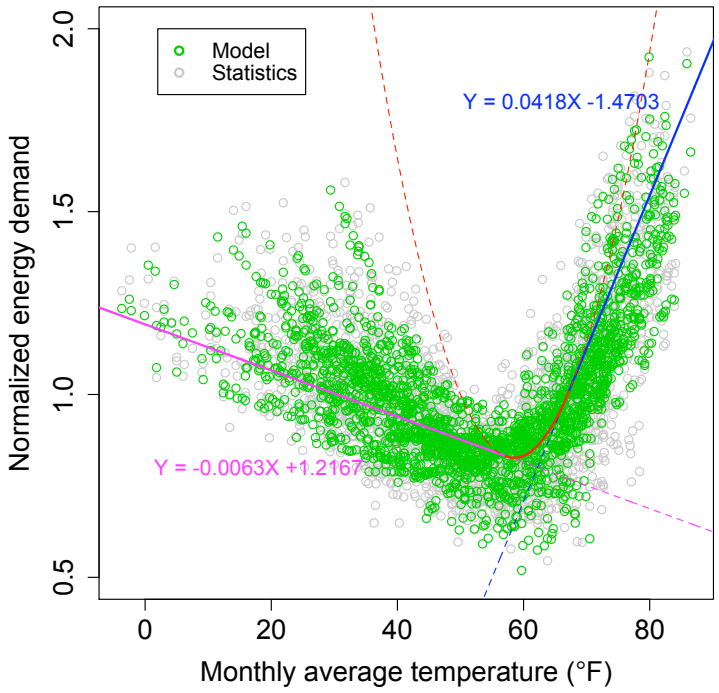

Figure 9. Global energy demand function derived from model estimates for US 50 state energy demands.

model calibration and green open circle shows energy demand estimates calculated by the calibrated model, respectively. The cross point of two lines (purple and blue) was derived from polynomial fitting performed separately from regression mentioned above. To connect two lines smoothly, hyperbola was applied (solid red curve in Figure 9). We calculated monthly factors to create monthly emission from annual total emission using the function. We calculated monthly energy demand using monthly temperature data and normalized the calculated monthly energy demand by annual total energy demand. The monthly emissions were obtained by multiplying monthly factors to annual total emission.

CONCLUSION

We created two 5 km x 5 km global maps of anthropogenic CO_2 emissions by integrating two surrogates of emission (population counts and nighttime lights data) and database of large point source. We treated emission attributed non-point sources separately by subtracting point source emission from the total emission. Since emissions from point sources account for significant proportions of national total emissions, our approach of using the CARMA dataset appears to be more effective in creating emission maps. The stable lights data has been rarely used in mapping of CO_2 emissions. However, the data is a promising surrogate to indicate exact locations of point sources. We also derived a relationship between temperature and energy demand to create monthly emission maps from annual total emissions. In a future study, we will evaluate our products by comparing with other emission estimates.

REFERENCES

Andres, R. J., G. Marland, I. Fung and E. Matthews, 1996. A 1˚ × 1˚ distribution of carbon dioxide emissions from fossil fuel consumption and cement manufacture, 1950-1990, *Global Biogeochem. Cycles*, **10** (3), 419-429

Andres, R. J., D. J. Fielding, G. Marland, T. A. Boden and N. Kumar, 1999. Carbon dioxide emissions from fossil-fuel use, 1751-1950, *Tellus*, 5**1B**, 759-765

Boden, T. A., G. Marland and R. J. Andres, 1995. Estimates of global, regional, and national annual CO_2 emissions from fossil-fuel burning, hydraulic cement production, and gas flaring: 1950-1992. ORNL/CDIAC-90, NDP-30/R6. Oak Ridge National Laboratory, U.S. Department of Energy, Oak Ridge, Tennessee.

Gurney, K. R., L. M. Rachel, A. S. Denning, P. J. Rayner, D. Baker, P. Bousquet, L. Bruhwiler, Y-H. Chen, P. Ciais, S. Fan, I. Y. Fung, M. Gloor, M. Heimann, K. Higuchi, J. John, T. Maki, S. Maksyutov, K. Masarie, P. Peylin, M. Prather, B. C. Pak, J. Randerson, J. Sarmiento, S. Taguchi, T. Takahashi, and C-W. Yuen, 2002. Towards robust regional estimates of CO_2 sources and sinks using atmospheric transport models, *Nature*, **415**, 626-630

IEA, 2007. CO_2 emissions from fuel combustion: 1971-2005 (2007 edition). International Energy Agency.

IPCC, 2009. Revised 1996 IPCC Guidelines for National Greenhouse Gas Inventories. IPCC/OECD/ IEA, Paris.

Marland, G., and R. M. Rotty, 1984. Carbon dioxide emissions from fossil fuels: A procedure for estimation and results for 1950-82, *Tellus*, **36**(B), 232-261

Marland, G., T. A. Boden, and R. J. Andres, 2008. Global, Regional, and National Fossil Fuel CO2 Emissions. In Trends: A Compendium of Data on Global Change. Carbon Dioxide Information Analysis Center, Oak Ridge National Laboratory, U.S. Department of Energy, Oak Ridge, Tenn., U.S.A.

Sailor, D. J. and C. Vasireddy, 2005. Correcting aggregate energy consumption data to account for variability in local weather, *Environmental Modelling & Software*, **21 (5)**, 733-738

United Nations, 2006. 2004 Energy Statistics Yearbook. United Nations Department for Economic and Social Information and Policy Analysis, Statistics Division, New York.

ACKNOWLEDGEMENT

Population counts and national boundary data of GPWv3 were provided by the Trustees of Columbia University in the City of New York, United Nations Food and Agriculture Programme (FAO), and the Centro Internacional de Agricultura Tropical (CIAT).

Key words
global CO_2 emission map, fossil fuel CO_2 emission, point source database, nighttime lights, monthly emission